STEM CELLS®

REGENERATIVE MEDICINE

Transplantation of Unique Subpopulation of Fibroblasts, Muse Cells, Ameliorates Experimental Stroke Possibly Via Robust Neuronal Differentiation

HIROKI UCHIDA,[a,b] TAKAHIRO MORITA,[a,b] KUNIYASU NIIZUMA,[b] YOSHIHIRO KUSHIDA,[c] YASUMASA KURODA,[c] SHOHEI WAKAO,[a] HIROYUKI SAKATA,[b] YOSHIYA MATSUZAKA,[d] HAJIME MUSHIAKE,[d] TEIJI TOMINAGA,[b] CESARIO V. BORLONGAN,[e] MARI DEZAWA[a,c]

Key Words. Cellular therapy • Pluripotent stem cells • Mesenchymal stem cells • Neuronal differentiation • Transplantation

ABSTRACT

Objective: Muse cells reside as pre-existing pluripotent-like stem cells within the fibroblasts, are nontumorigenic, exhibit differentiation capacity into triploblastic-lineage cells, and replenish lost cells when transplanted in injury models. Cell fate and function of human skin fibroblast-derived Muse cells were evaluated in a rat stroke model. Methods: Muse cells (30,000), collected by pluripotent surface marker stage-specific embryonic antigen-3, were injected stereotaxically into three deposits within the rat ischemic cortex at 2 days after transient middle cerebral artery occlusion, and the cells' biological effects were examined for more than 84 days. Results: Muse cells spontaneously and promptly committed to neural/neuronal-lineage cells when cocultured with stroke brain slices. Muse-transplanted stroke rats exhibited significant improvements in neurological and motor functions compared to control groups at chronic days 70 and 84, without a reduction in the infarct size. Muse cells survived in the host brain for up to 84 days and differentiated into NeuN (~65%), MAP-2 (~32%), calbindin (~28%), and GST-π (~25%)-positive cells in the cortex, but glial fibrillary acidic protein-positive cells were rare. Tumor formation was not observed. Muse cells integrated into the sensory-motor cortex, extended their neurites into cervical spinal cord, and displayed normalized hind limb somatosensory evoked potentials. Interpretation: Muse cells are unique from other stem cells in that they differentiate with high ratio into neuronal cells after integration with host brain microenvironment, possibly reconstructing the neuronal circuit to mitigate stroke symptoms. Human fibroblast-derived Muse cells pose as a novel source of transplantable stem cells, circumventing the need for gene manipulations, especially when contemplating autologous cell therapy for stroke. STEM CELLS *2015; 00:000–000*

INTRODUCTION

Stem cell transplantation has been designed fundamentally as a cell replacement approach [1, 2], but to date many neural transplantation studies have not been successful in demonstrating good graft survival and long-term engraftment. Although mesenchymal stem cells (MSCs), particularly those derived from bone marrow (BM), are easy accessible and have established safety profiles in stroke preclinical studies and clinical trials, therapeutic outcomes have been inconclusive thus far because of modest functional recovery likely due to low rate of neuronal cell replenishment [3–6]. An alternative cell therapy mechanism advances the notion of grafted cells' by-stander effects, in that cytokines produced by transplanted MSCs may rescue dying and spared cells toward self-repair, and modulate inflammatory reactions [7]. However, the endogenous regenerative effects may not be sustained because graft persistence, and the graft's secreted factors, in the host tissue do not persist over time [8]. The search for a transplantable cell with high potential of graft survival and engraftment has focused particularly on autologously derived stem cells. Induced pluripotent stem (iPS) cells might also be one of cell sources for treating stroke patients due to the availability of autologous mature cells such as skin fibroblasts [9]. Unfortunately, however, iPS cells are consistently obtained only after introduction of exogenous genes including oncogenic factors into the cells [9], raising safety concerns, such as the possibility of tumor formation, when using

[a]Department of Stem Cell Biology and Histology; [b]Department of Neurosurgery; [c]Department of Anatomy and Anthropology; and [d]Department of Physiology, Tohoku University Graduate School of Medicine, Sendai, Japan; [e]Department of Neurosurgery and Brain Repair, University of South Florida College of Medicine, Tampa, Florida, USA

Correspondence: Mari Dezawa, Ph.D., M.D., Department of Stem Cell Biology and Histology, Tohoku University Graduate School of Medicine, 2-1 Seiryo-machi, Aoba-ku, Sendai, Miyagi 980-8575, Japan. Telephone: +81-22-717-8025; Fax: +81-22-717-8030; e-mail: mdezawa@med.tohoku.ac.jp; or Cesar V. Borlongan, Ph.D., Department of Neurosurgery and Brain Repair, Center of Excellence for Aging and Brain Repair, University of South Florida College of Medicine, 12901 Bruce B Downs Blvd, Tampa, Florida 33612, USA. Telephone: 813-974-3988; Fax: 813-974-3078; e-mail cborlong@health.usf.edu

Received May 27, 2015; accepted for publication July 12, 2015; first published online in STEM CELLS *EXPRESS* September 21, 2015.

1066-5099/2015/$30.00/0

http://dx.doi.org/10.1002/stem.2206

these cells for transplantation therapy. Furthermore, induction into neuronal-lineage cells in cell processing center prior to transplantation is inevitable in iPS cells for clinical use in stroke patients.

Multilineage-differentiating stress-enduring (Muse) cells, a unique stem cell population that are able to self-renew and differentiate into cells representative of all three germ layers from a single cell and are stress tolerant, were identified in mesenchymal tissues such as the BM, adipose tissue, and dermis, as well as in cultured fibroblasts, as cells positive for pluripotent surface marker, stage-specific embryonic antigen (SSEA)−3 [10]. Since they normally reside in adult mesenchymal tissues, they are not tumorigenic [10–12]. Muse cells possess unique characteristics that distinguish them from other multipotent/pluripotent stem cells; intravenously injected BM-derived Muse cells migrate to and integrate into damaged tissues and spontaneously differentiate into functional cells in damaged models of the liver, muscle, and skin [10]. Locally injected adipose tissue-derived Muse cells accelerate tissue reconstruction in skin ulcers of a diabetes mellitus model by newly replenishing dermal and epidermal cells and BM-Muse cells were shown to replenish new neuronal cells in a stroke model [13, 14]. All these experiments used naive Muse cells solely after SSEA-3 screen collection, and neither the introduction of exogenous genes for resetting the cells nor the induction of the cells to make them commit into specific lineages has been implemented before transplantation.

Muse cells display high efficiency for differentiating into neuronal cells, such as cells positive for neurofilament and microtubule-associated protein (MAP)−2, under cytokine induction, but more importantly these cells spontaneously attain the phenotype of the host microenvironment, indicating their potential applicability for stroke therapy [10–12, 15]. Based on the availability of pluripotent-like Muse cells from the skin and cultured fibroblasts in the absence of oncogenic factor introduction, and in line with our efforts to advance autologous cell transplantation, here we focused on assessing cell fate and function of human skin fibroblast-derived Muse cells following transplantation in a rodent stroke model.

Materials and Methods

Cell Preparation and Characterization

Muse cells and non-Muse cells, as control, were separated from normal human dermal fibroblasts (NHDFs) derived from adult skin purchased from Lonza, Inc. (Allendale, NJ, http://www.lonza.com), as previously described [10]. NHDFs from the 8th to 14th subcultures were used in this study. Muse cells were isolated from NHDFs with a fluorescence-activated cell sorter (FACS; Aria II, Becton Dickinson, Franklin Lakes, NJ, http://www.bd.com/) using an anti-SSEA-3 antibody (1:50; MAB4303, Millipore, Temecula, CA, http://www.merckmillipore.com/) detected by fluorescein isothiocyanate (Supporting Information Fig. S1A, gate P3). We also collected ∼5% of cells with the lowest SSEA-3 expression as non-Muse cells (Supporting Information Fig. S1A, gate P6).

A cluster formation assay in a single-cell suspension culture (for 7 days) was performed as previously described [10]. The formed clusters were individually transferred onto gelatin-coated 24-well dishes, and cells were allowed to expand from the adhered clusters for 14 days. Cells were fixed with 4% paraformaldehyde in phosphate buffer saline (PBS), washed, and incubated with blocking solution containing 20% blockAce (UK-B40, DS Pharma, Osaka, Japan, http://www.ds-pharma.co.jp/), 5% bovine serum albumin (A9418, Sigma-Aldrich, St. Louis, MO, http://www.sigmaaldrich.com/), and 0.3% Triton X-100 (160-24755, Wako, Osaka, Japan, http://www.wako-chem.co.jp/) in 0.02 M PBS. They were then stained with anti-neurofilament-M rabbit IgG (1:200; AB1987, Millipore) as an ectodermal marker, anti-smooth muscle actin mouse IgG (1:200; MS-113-P0, Thermo-Fisher Scientific, Waltham, MA, http://www.thermofisher.com/) as a mesodermal marker, and anti-cytokeratin 7 mouse IgG (1:100; MAB3226, Millipore) as an endodermal marker. Furthermore, to confirm the spontaneous neural differentiation ability of the clusters, the expanded cells were further incubated with anti-nestin mouse IgG (1:200; MAB5326, Millipore), anti-MAP-2 rabbit IgG (1:20; 6242-0039, AbD Serotec, Raleigh, NC, http://www.abdserotec.com/), anti-glial fibrillary acidic protein (GFAP) rabbit IgG (1:500; IR524, DAKO, Carpinteria, CA, http://www.dako.com/), and anti-O4 mouse IgG (1:50, MAB345, Millipore). All samples were followed by incubation with secondary antibodies either of Alexa Fluor 488 (1:500; A21202, Life Technologies, Waltham, MA, http://www.thermofisher.com/) or Alexa Fluor 568 (1:500; A10037, Life Technologies)-conjugated donkey anti-mouse IgG, and Alexa Fluor 488 (1:500; A21206, Life Technologies) or Alexa Fluor 568 (1:500; A10042, Life Technologies)-conjugated donkey anti-rabbit IgG, and were inspected under laser confocal microscope (Nikon, Tokyo, Japan, http://nikon.co.jp/).

Induction of Transient Focal Cerebral Ischemia

All animal experiments were approved by the Animal Care and Experimentation Committee of the Tohoku University Graduate School of Medicine. Transient focal cerebral ischemia was induced in 10-week-old male Wistar rats under deep anesthesia by intraluminal middle cerebral artery occlusion (MCAo) with a commercially available suture (4035PKRe5, Doccol, Corp., Sharon, MA, http://www.doccol.com/) for 60 minutes, as previously described [16, 17].

Cell Transplantation

NHDFs were introduced with lentivirus green fluorescent protein (GFP) for labeling human Muse and non-Muse cells, as described [16], and then Muse and non-Muse cells were collected by SSEA-3 staining.

Two days after MCAo, all rats were scored using the modified neurologic severity score (mNSS) [3]. mNSS was composed of five tests as follows: (a) elevating rat by the tail (0–3 points), (b) placing rat on the floor (0–3), (c) sensory tests (0–2), (d) beam balance tests (0–6), and (e) reflexes absent and abnormal movements (0–4). The following severity scale was used, namely 13–18 indicated severe injury; 7–12, moderate injury, and; 1–6, mild injury [3]. Rats that scored 7–13 were selected for transplantation. Animals were fixed on a stereotaxic apparatus (SR-6R, Narishige, Tokyo, Japan) under general anesthesia. Muse cells (Muse group), non-Muse cells (non-Muse group), and the same volume of PBS (vehicle group) were transplanted using a 2.0-μl Hamilton microsyringe (7002KH, Hamilton, Co., Reno, NV, http://www.hamiltoncompany.com/) for more than ∼5 minutes. Rats were injected

with a total of 30,000 viable cells or the same volume of PBS; the cells were injected as three deposits (10,000 cells/2 μl per each deposit) in PBS directly into the ischemic border zone (a) (from bregma: anterior (A) +2.0 mm, right (R) +2.0 mm, ventral (V) +4.0 mm), (b) (from bregma: A −1.0 mm, R +3.0 mm, V +4.5 mm), (c) (from bregma: A −4.0 mm, R +3.0 mm, V +4.5 mm) [17]. The incisor bar was set to −3.3 mm. Ten animals were used for behavioral analysis for each group (Muse, non-Muse, and vehicle). Five out of ten animals were randomly chosen at day 84 and subjected to electrophysiological study, and remainder of animals to histologic analysis. Retrograde tracing and histologic analysis with GFP-labeled Muse and non-Muse cell transplantation were performed independently from behavioral analysis with four animals from each group, respectively.

The immunosuppressive agent FK506 (Astellas Pharma, Inc., Osaka, Japan, http://www.astellas.com/) was administered intraperitoneally (0.5 mg/kg) immediately after the transplantation in all three groups including the vehicle group, daily for the first 14 days, and every other day for the next 10 weeks with the same dose, as previously described [18].

Behavioral Analysis

The severity of the neurologic damage was evaluated based on the mNSS and rotarod test [3]. Behavioral assessments were performed at −2 (before MCAo), 7, 14, 21, 28, 42, 56, 70, and 84 days after transplantation by an investigator blinded to the experimental groups.

The rotarod test was performed with MK-630B (Muromachi Kikai, Co., Tokyo, Japan, http://www.muromachi.com/). The cylinder speed was slowly increased from 4 to 40 rpm for more than 5 minutes. A trial ended if the animal fell off the cylinder. Rats were trained for 5 days before MCAo. The mean duration on the device was recorded with two measurements just before surgery for the baseline score, and the results are presented as a percentage of the mean duration (two trials) on the rotarod compared with the internal baseline control (before surgery).

Histologic Analysis

On day 84 after transplantation, all animals were fixed with periodate lysine paraformaldehyde (PLP) solution (0.01 M $NaIO_4$, 0.075 M lysine, 2% paraformaldehyde, pH 6.2) under deep anesthesia. Excised brains were cut coronally with feather knives and a brain slicer (MK-RC-01, Muromachi Kikai, Co., Japan) at 3-mm intervals to match the sites where the cells had been transplanted. Each slice was then further cut into 10-μm thick sections using a cryostat (CM1850; Leica, Wetzlar, Germany, http://www.leicabiosystems.com/).

Samples were stained with hematoxylin and eosin (H&E) and examined with fluorescent immunohistochemistry. Infarct volume was calculated as the sum of lesion areas of the five H&E-stained slices, and tumorigenicity was also evaluated by H&E staining, as previously described [19]. The presence of engrafted cells in the infarcted brain and evaluation of their differentiation into neural-lineage were assessed with fluorescent immunohistochemistry using antibodies against human mitochondria (hMit) (1:100; ab3298, Abcam, Cambridge, England, http://www.abcam.com/), GFP (1:1,000; ab6673, Abcam), NeuN (1:200; MAB377, Millipore), MAP-2 (1:1,000; M1406, Sigma), Calbindin (1:500; AB1778, Millipore), GST-π (1:500; 312, MBL, Aichi, Japan, http://www.mbl.co.jp/), GFAP (1:500; IR524, DAKO), and synaptophysin (1:1,000, MAB5258, Millipore). The samples were then incubated either with anti-mouse IgG and anti-rabbit IgG secondary antibodies conjugated with Alexa Fluor-488 or −546, counter stained with 4′,6-diamidino-2-phenylindole staining (1:1,000; D9542, Sigma) and inspected under laser confocal microscopy (Nikon). All the hMit(+) or GFP(+) cells were counted with Image-J, as previously described [20].

Retrograde Tracing

Retrograde tracer labeling with a fluorogold was performed according to a previous report [16]. On day 84, the rats received an injection of 0.1 μl of 4% fluorogold (Biotium, Hayward, CA, https://biotium.com/) into the contralateral dorsal funiculus of cervical spinal cord (C1 level) through a Hamilton microsyringe (7002KH, Hamilton, Co.) under general anesthesia. Seven days later (day 91), fluorogold-positive GFP(+)-human cells were detected at the ipsilateral motor cortex.

Electrophysiology

At day 84 after transplantation, hind limb somatosensory evoked potentials (SEP) were measured in transplanted animals ($n = 5$ for Muse and vehicle groups). All rats were anesthetized with an intraperitoneal injection of 60 mg/kg ketamine and 15 mg/kg xylazine, and administered additional 12 mg/kg ketamine and 3 mg/kg xylazine every 30 minutes to maintain the anesthesia. Hind limb SEP was measured from the primary somatosensory area of the infarct side (from bregma: A −2.5 mm, R +2.5 mm, V +1.0 mm, incisor bar −3.3 mm) with a 0.25-mm glass-coated elgiloy electrode (1 MΩ) and power lab system (AD Instruments, Dunedin, New Zealand, http://www.adinstruments.com/), as previously described [21]. The reference electrode was placed on the cerebellum. Electrical stimulation delivered to contralateral quadriceps muscle comprised 100 serial biphasic pulses (10 mA, 200 ms duration, 1 Hz), generated by a digital stimulator (SEN-8203, Nihon Kohden, Corp., Tokyo, Japan, http://www.nihonkohden.co.jp/) and an isolator (SS-104J, Nihon Kohden, Corp.). We measured and averaged 100 serial signals (amplified 1,000 times, and filtered [band pass 5–3,000 Hz]). We analyzed the peak latency and amplitude of the first wave observed after the stimulation. Both are presented as the ratio to the contralateral (normal side).

Observation of Muse Cells in the Stroke Brain Slice

MCAo was made in CB17/Icr-Prkdc<scid>/CrlCrlj severe combined immunodeficiency (SCID) mice. Two days after, brain slices of the ipsilateral side at 2-mm-thick were prepared and 30,000 of GFP^+-human Muse cells were cocultured to each brain slice. Culture media contained FluoroBrite-Dulbecco's modified Eagle's medium (Gibco, waltham, MA, http://www.thermofisher.com/), GlutaMAX (Gibco), 0.1 mg/ml kanamycin sulfate (Gibco), and 10% fetus bovine serum in an atmosphere containing 5% CO_2 at 37°C. Three and seven days after, samples were analyzed by RT-PCR and multiphoton confocal microscope (Nikon, A1RNP). After observation under multiphoton confocal microscope, samples were fixed with 4% paraformaldehyde, cryosections at 8-μm thick were prepared and stained with primary antibodies either of NeuroD (1:100, ab60604, Abcam), MAP-2 (1:1,000; M1406, Sigma), and NeuN

(1:200; MAB377, Millipore), followed by secondary antibodies anti-mouse or rabbit IgG conjugated with Alexa Fluor-546, and inspected under laser confocal microscope (Nikon).

RT-PCR. Total RNA was extracted from cells and purified using the RNeasy mini kit (QIAGEN, Venlo, Nederland, http://www.qiagen.com/). First-strand complementary DNA was synthesized using SuperScript III reverse transcriptase (Invitrogen, Waltham, MA, http://www.thermofisher.com/). The PCR was performed using Ex Taq DNA polymerase using standard temperature cycling conditions. PCR was carried out using specific primers designed for each gene as follows: (a) human beta actin sense 5′-CATTAAGGAGAAGCTGTGCTAC-3′ and antisense 5′-GATCTTCATTGTGCTGGGT-3′, (b) mouse beta actin sense 5′-ACCCTAAGGCCAACCGTGAAAAGATGA-3′ and antisense, 5′-CCGCTCGTTGCCAATAGTGATGACCT-3′, (c) human Mash1 sense 5′-ACTTTGGAAGCAGGGTGAT-3′ antisense 5′-ACTGCACTTTAAGAAAGGGC3′, (d) human Doublecortin (DCX) sense 5′-GAGTGCTCAGAGTCCAGAGT-3′, antisense 5′-GGACTAGCACATTTTGCATC-3′, and (e) human MAP-2 sense 5′-GCACTGATGATAAAGTTCGAA-3′ and antisense 5′-GATGCATCTGTTGGTATTGA-3′.

Statistics

Data are expressed as median for the mNSS and mean ± SD for the other experiments. Statistical analyses were performed using JMP 10 software (SAS Institute, Inc., Cary, NC, http://www.sas.com). The mNSS and rotarod test were analyzed using one-way repeated measure analysis of variance, followed by Dunn's post hoc test for the mNSS and Tukey-Kramer's post hoc test for the rotarod test. Stroke volume and SEP latency were analyzed with one-way factorial analysis of variance and Tukey-Kramer's post hoc test. Comparison of the engrafted cells was analyzed with Student's *t* test, while SEP was analyzed using ANOVA and post hoc pairwise comparisons. A value of $p < .05$ was considered significant.

Results

Differentiation Capacity of Muse Cells into Neural Linage Cells In Vitro

As described previously, we separated NHDFs into SSEA-3^{+}-Muse cells and SSEA-3^{-}-non-Muse cells by FACS (Supporting Information Fig. S1A) [10–12, 15]. The Muse cells comprised 5.07% ± 1.25% of the NHDF. Both Muse and non-Muse cells were further subjected to single-cell suspension culture, and confirmed that only single Muse cells formed characteristic clusters similar to embryonic stem cell (ESC)-derived embryoid bodies (Supporting Information Fig. S1B), whereas none of the non-Muse cells formed clusters. As reported previously, expression of pluripotency markers, Oct3/4, Nanog, and Sox2 were confirmed in these clusters (not shown) [10–12, 15]. We then transferred single Muse cell-derived clusters individually onto gelatin-coated dishes to allow cells to expand from adhered single-Muse cell-derived cluster (Supporting Information Fig. S1C). Differentiation of expanded into triploblastic-lineage cells was reproduced (Supporting Information Fig. S1D) [10–12, 15]. Cells expanded from single Muse cell-derived clusters on gelatin-coated culture dishes also expressed the neural markers nestin (∼1.9%), MAP-2 (∼3.8%), GFAP (∼3.4%), and O4 (∼2.9%), suggesting the ability of Muse cells to spontaneously differentiate into neural-lineage cells (Supporting Information Fig. S1F). Since non-Muse cells do not form single-cell-derived clusters, they were directly plated to gelatin-coated dish and culture for the same period, while none of the cells expressed any of the above markers (not shown).

Muse Cells Improve Behavioral Functions at the Chronic Stage of Stroke

Stroke rats received stereotaxic transplantation of either human Muse (Muse group), non-Muse cells (non-Muse group) (both groups received 10,000 cells/2 μl for each deposit for three cortical coordinates; 30,000 cells injected totally), or the same volume of PBS (vehicle group) into the ischemic boundary zone of the rat brain 2 days after stroke onset.

Infarct size, assessed by ratio of the volume in ipsilateral to contralateral hemispheres in H&E staining at 84 days after transplantation, was almost the same among Muse, non-Muse, and vehicle groups, and there were no significant statistical differences among the three groups (Fig. 1A, 1B). No signs of tumor formation were observed in any of the rats in all three groups. Interestingly, when the number of nuclei per area was counted in the peri-infarct area, the Muse group displayed higher number with statistically significant difference compared to the vehicle group ($p < .05$) (Fig. 1C). However, there were no statistical differences between the Muse and non-Muse groups in peri-infarct area, nor among the three groups in sensorimotor cortex (Fig. 1C).

We next investigated whether transplantation of Muse cells could facilitate functional recovery in stroke by monitoring neurologic performance with the mNSS and rotarod test (Fig. 2A, 2B). The mNSS and rotarod test results were not significantly different among the three groups until day 56. Notably, however, substantial recovery in the Muse group was observed at days 70 and 84 in both the mNSS and rotarod test. The mNSS in the Muse group indicated substantial and significant recovery compared to the non-Muse ($p < .001$) and vehicle ($p < .001$) groups at day 70, and this improvement was maintained at day 84 (Muse vs. non-Muse, $p < .001$ and Muse vs. vehicle, $p < .01$) (Supporting Information Movies; "behavior day 84 Muse group" and "behavior day 84 non-Muse group"). Similarly, at days 70 and 84, the rotarod test revealed substantial recovery in the Muse group compared to the non-Muse (both at days 70 and 84; $p < .01$) and vehicle (day 84; $p < .01$) groups. Importantly, statistical difference was not observed between the non-Muse and vehicle groups at any time point in either the mNSS or rotarod test.

Survival of Muse Cells in the Stroke Brain for 84 Days

Survival of transplanted Muse and non-Muse cells in the host brain at day 84 was examined by immunohistochemistry. Cells positive for human marker, hMit, were detected extensively in the area of the peri-infarct area in the Muse group (Fig. 3A–3C). In sharp contrast, the number of hMit(+) cells was scarcely detectable in non-Muse group, suggesting that majority of the grafted non-Muse cells were excluded from the host brain by day 84 after transplantation (Fig. 3B, 3D). The number of hMit(+) cells was significantly greater in the Muse group compared with the non-Muse groups at every point from +5 through −7 mm from the bregma (Fig. 3B).

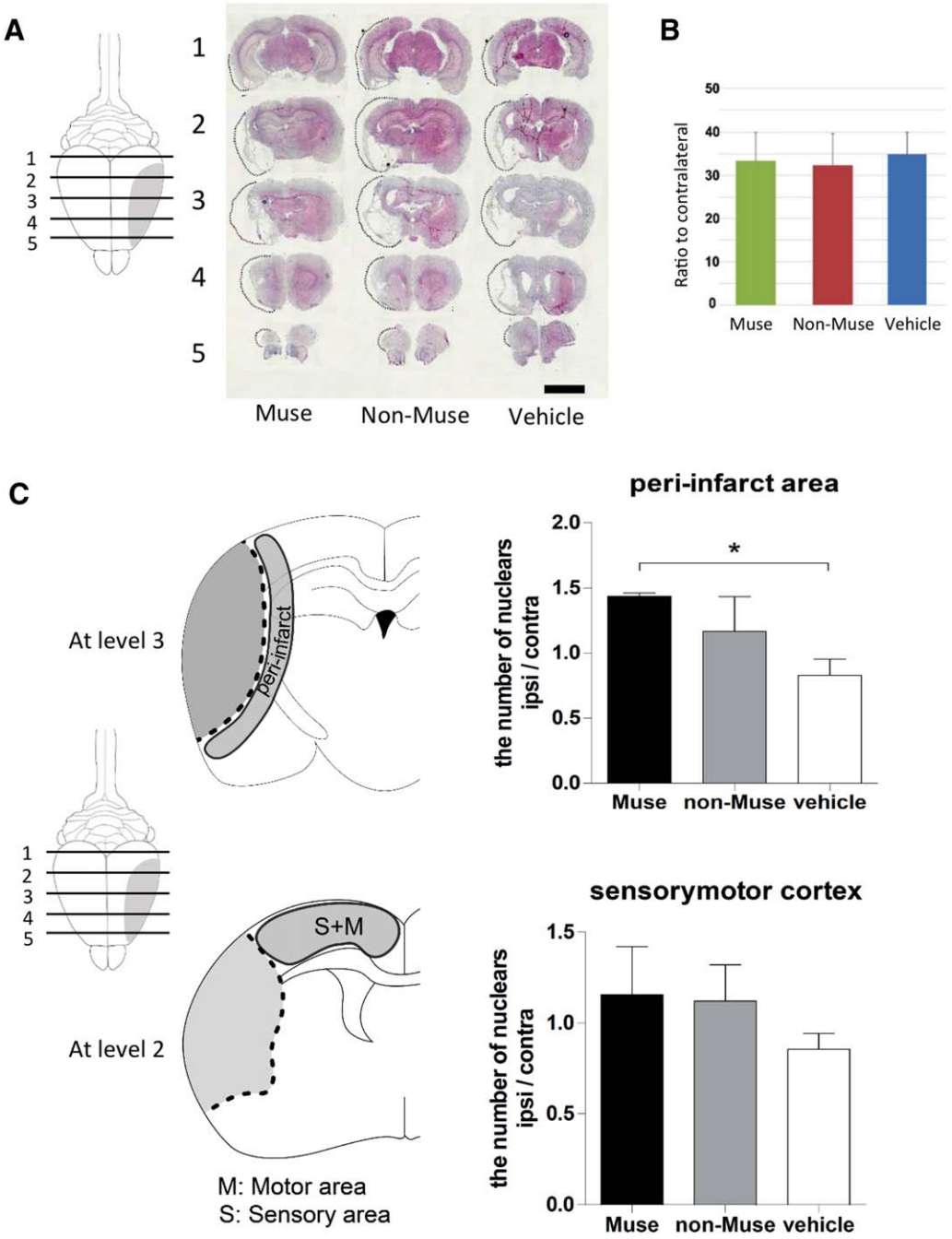

Figure 1. Infarct size and nuclei number in the ipsilateral cortex (84 days). **(A)**: Representative brain splices at different levels of the Muse, non-Muse, and vehicle groups stained with H&E. Bar = 1 mm. **(B)**: Measurement of infarct size based on H&E staining. Infarct size did not differ significantly among three groups. **(C)**: Counting of nuclei per area by 4′,6-diamidino-2-phenylindole staining in the peri-infarct area at level 3 and in the sensory-motor cortex at level 2 among three groups. *$p < 0.05$.

Differentiation of Muse Cells in the Stroke Brain

Because survival of transplanted human cells in the host brain was observed in the Muse group, but not in the non-Muse group, further immunohistological analysis was implemented in the peri-infarct area of the Muse group at day 84. Cells positive for general neuronal markers, NeuN and MAP-2, were $64.6\% \pm 0.6\%$ and $32.4\% \pm 2.4\%$ of GFP^+ cells, respectively, and for interneuron marker, calbindin, was $27.5\% \pm 2.5\%$ (Fig. 4A–4C, 4E). As for glial markers, oligodendrocyte marker, GST-π, were $25.0\% \pm 0.8\%$ positive in GFP^+ cells (Fig. 4D), while GFAP+ cells could only be scarcely detected (Fig. 4E).

Retrograde Labeling Study

As mentioned above, the number of nuclei in the ipsilateral sensory-motor cortex was slightly elevated in the Muse group compared to the vehicle group (Fig. 1C), suggesting incorporation of transplanted Muse cells into the motor cortex. We then investigated whether integrated Muse cells committed to the pyramidal tract. Retrograde tracer, fluorogold, injected

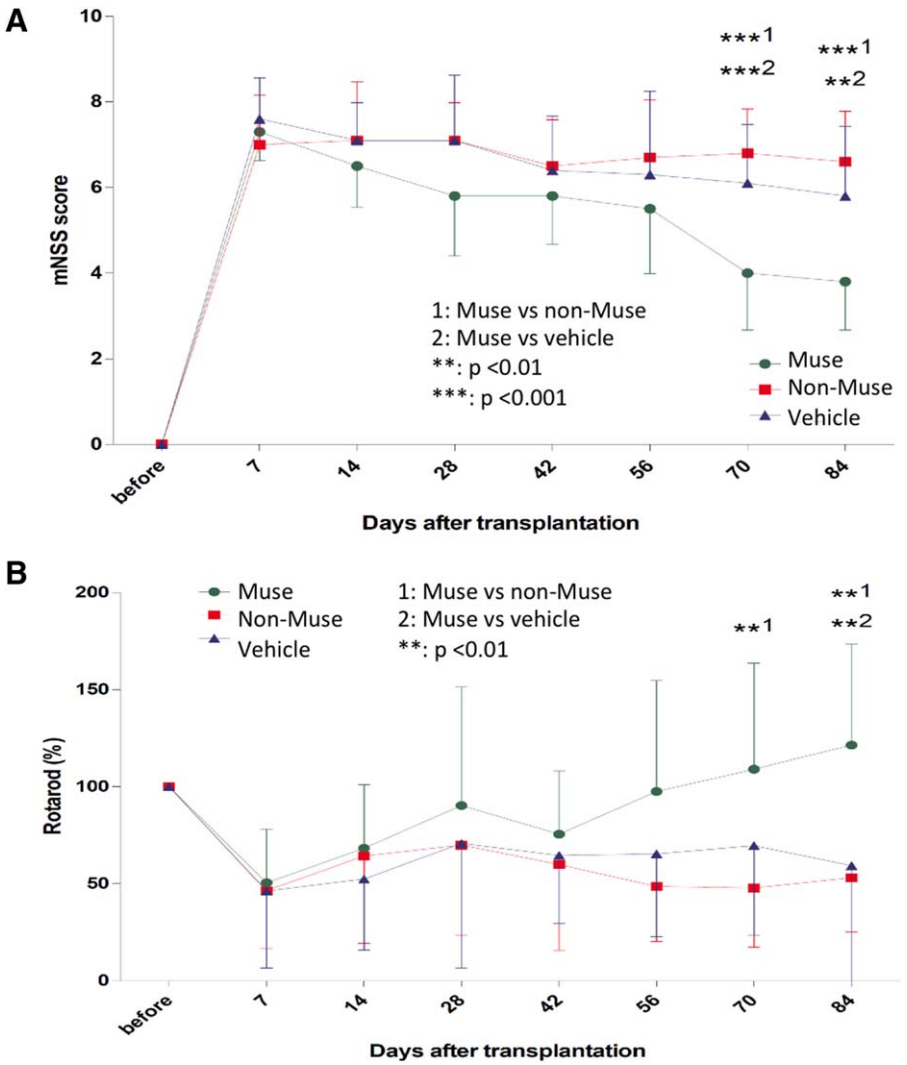

Figure 2. Behavioral performance. Transplantation of Muse cells resulted in substantial functional recovery in mNSS **(A)** and rotarod test **(B)** at the chronic stage of stroke after day 70. Videos for the both Muse and non-Muse groups at day 84 are provided in Supporting Information Movies. Abbreviation: mNSS, modified neurologic severity score.

into the contralateral dorsal funiculus of C1 level spinal cord at day 84 retrogradely labeled some of GFP+ cells in the ipsilateral motor cortex 7 days after the injection (Fig. 5A–5C). This suggests that human Muse cells integrated into the motor cortex extended neurites into the pyramidal tract, at least to C1 level of the spinal cord.

Electrophysiological Assessment

Integration of GFP$^+$-human Muse cells was also recognized in the ipsilateral sensory cortex (Fig. 6A). Furthermore, synaptophysin was detected adjacent to dendrite-like processes belonging to GFP$^+$-human Muse cells in the sensory cortex (Fig. 6B). These suggest that Muse cells that integrated into the sensory cortex were involved in sensory neural circuit.

We then assessed possible electrophysiological improvements in the Muse group compared to the vehicle and non-Muse groups. Bilateral hind limb SEPs were recorded at the primary sensory cortex 84 days after transplantation (Fig. 6C). ANOVA revealed significant treatment effects in amplitude ($p < .05$), but not in latency ($p > .05$) (Fig. 6C–6E). Post hoc pairwise comparison revealed that Muse cell-transplanted stroke animals displayed significantly higher amplitude than vehicle-treated stroke animals ($p < .05$) (Fig. 6C, 6E). Muse cell transplanted stroke animals also showed a trend of higher amplitude than non-Muse cell transplanted stroke animals but the difference between the two groups did not reach significance ($p = .11$) (Fig. 6C, 6E). The non-significant trend of increased amplitude in Muse cell transplanted stroke animals compared to non-Muse cell transplanted stroke animals could be due to small sample size. Nonetheless, the lack of significance between non-Muse cell transplanted stroke animals and vehicle-treated stroke animals suggests that the significant treatment effects were likely produced by the higher amplitude exhibited by Muse cell transplantation.

Reaction of Muse Cells to Stroke Microenvironmental Cues

Muse cells spontaneously differentiate into cell phenotypes compatible to the tissue they homed under pathological condition [10] prompted us to investigate whether Muse cells similarly respond to stroke brain microenvironmental cues. To

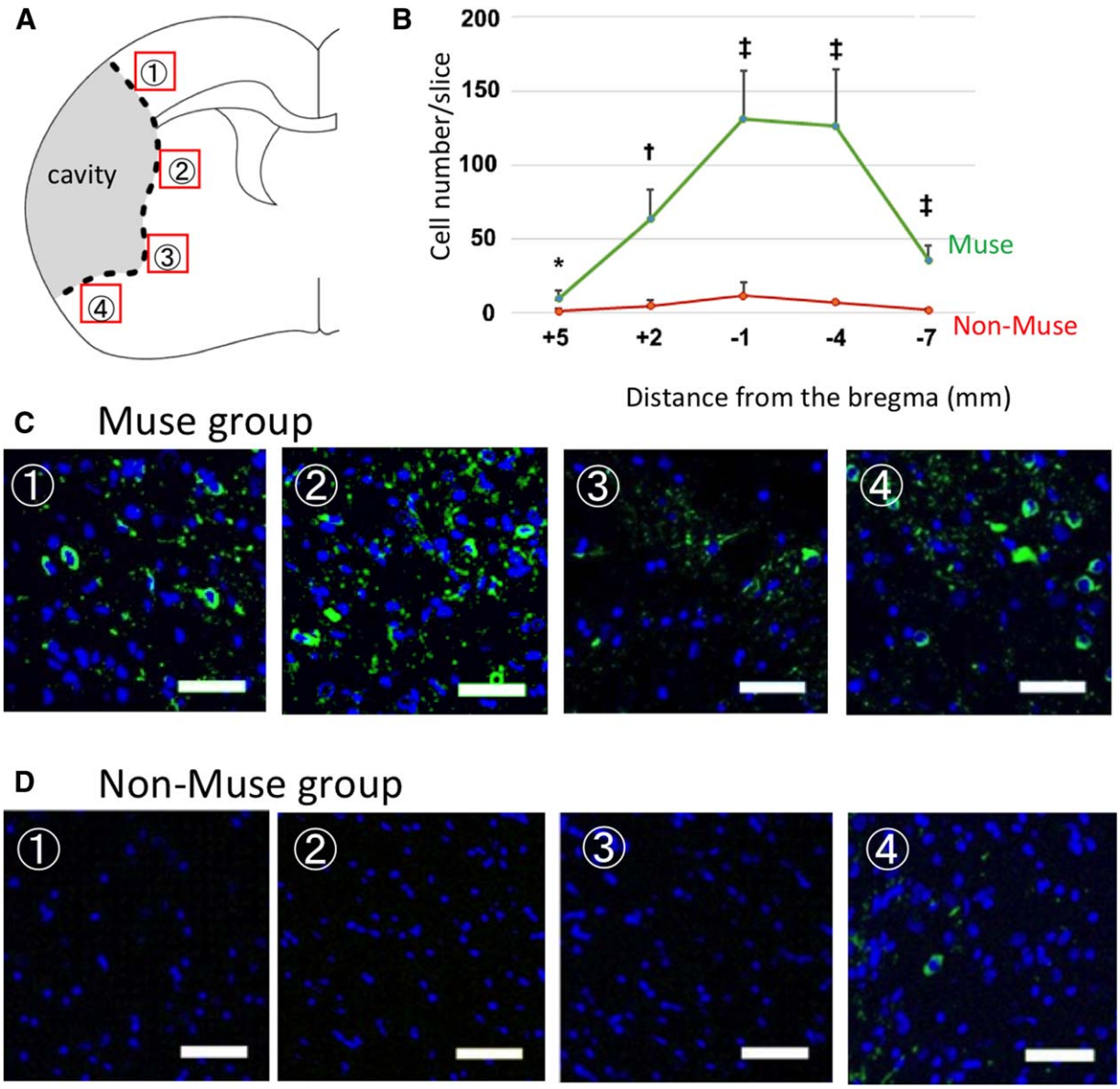

Figure 3. Survival of grafted cells in the peri-infarct area. **(A)**: Schematic figure indicating the area counted for hMit+ cells. **(B)**: Quantification of the number of grafted cells 84 days after transplantation. Specimens were picked up every 3 mm and the number of hMit(+) cells was counted. A significantly greater number of grafted cells was detected in the Muse group. *, $p < .05$; †, $p < .01$; ‡, $p < .001$. **(C, D)**: Detection of human Muse (C) and non-Muse cells (D) by hMit immunostaining revealed substantial incorporation of the grafted Muse cells in the peri-infarct area at 84 days after transplantation, whereas a negligible number of non-Muse cells was detected in the same region. Nuclei were counterstained with 4′,6-diamidino-2-phenylindole (blue). Scale bar = 50 μm.

analyze the reaction of Muse cells when they were exposed to the microenvironment of stroke tissue, we conducted an in vitro experiment by coculturing human GFP$^+$-Muse cells with brain slices harvested from stroke SCID mouse and observed under multiphoton confocal microscopy. At day 3, GFP$^+$-Muse cells incorporated already into the brain slices and started to extend neurite-like processes, with some of these outgrowths even penetrating into the tissue for up to 60 μm (Fig. 7A, 7B, Supporting Information Movie "d3-infarct area"). Expression of NeuroD and human Mash1 was recognized in these cells (Fig. 7C, 7E). At day 7, GFP$^+$-Muse cells that were incorporated into the brain slices displayed extensions of neurite-like processes more abundantly, started to form elaborate connections and networks with each other, and expressed human MAP-2, NeuN, and human DCX (Fig. 7D, 7E, Supporting Information Movie "d7-infarct area"). Notably, incorporation of Muse cells or morphological changes such as neurite extension was scarcely seen when cells were cocultured with intact area (Fig. 7A, Supporting Information Movie "d7-intact area"). Additionally as control, we cocultured brain slices with non-Muse cells, which exhibited no detectable expression of human Mash1, human MAP-2 or human DCX at either day 3 or day 7 in culture (Fig. 7E).

Discussion

This study is the first to show that human skin fibroblast-derived Muse possessed inherent ability to assume stemness

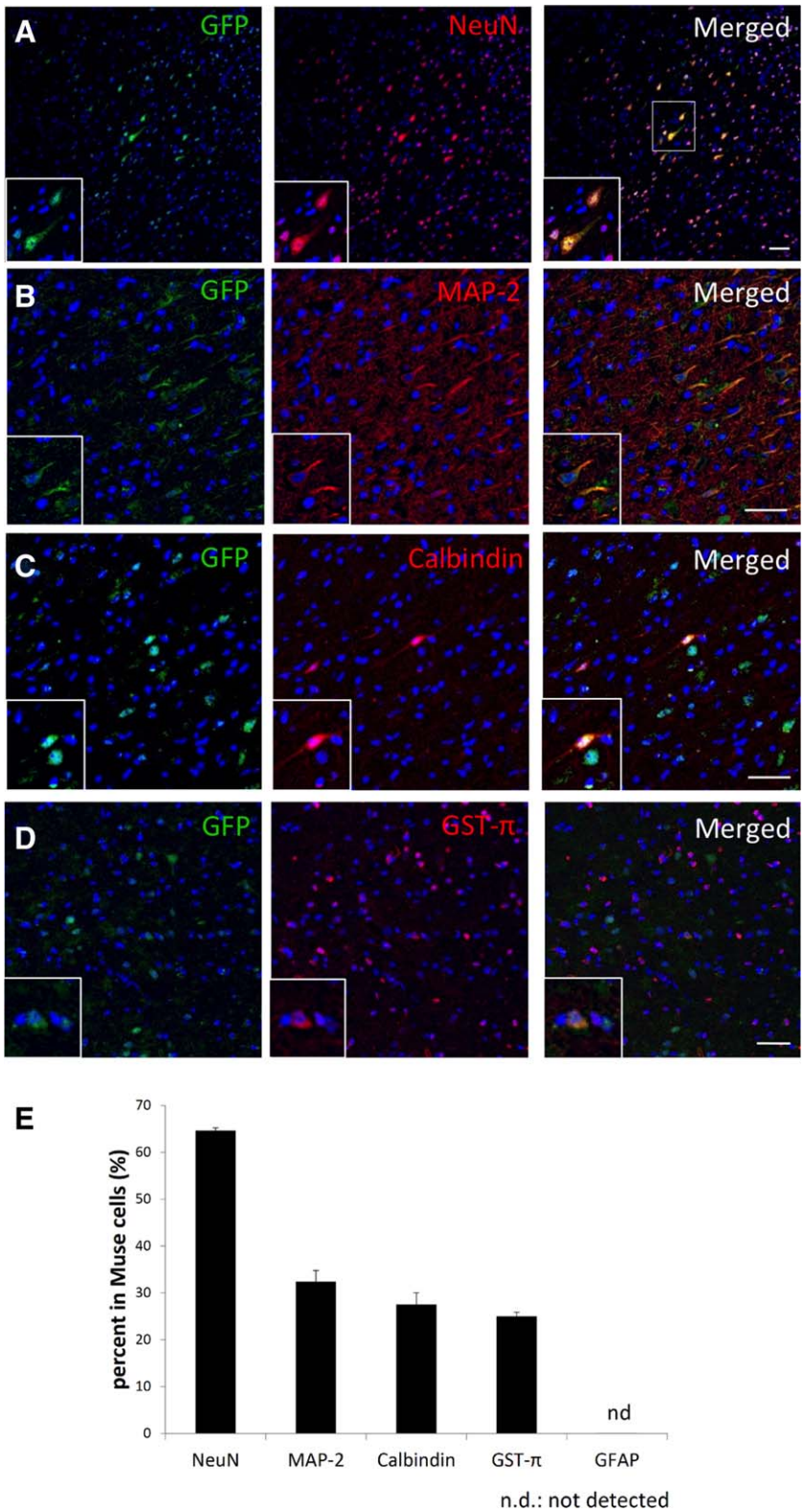

Figure 4. Differentiation of Muse cells in the peri-infarct area 84 days after transplantation. The grafted GFP+-Muse cells differentiated into NeuN **(A)**, MAP-2 **(B)**, calbindin **(C)**, and GST-π **(D)**. Scale bar = 50 μm. **(E)**: The percentage of each markers in GFP+ cells. Abbreviations: GFAP, glial fibrillary acidic protein; GFP, green fluorescent protein.

properties and to readily differentiate into neural-lineage cells after integration into the stroke brain in vivo. Such ease in Muse cell in vivo-differentiation was achieved in the absence of oncogenic factor-induction regimen and the expedited commitment to neural phenotype was specifically in response to stroke microenvironment. Muse cells that

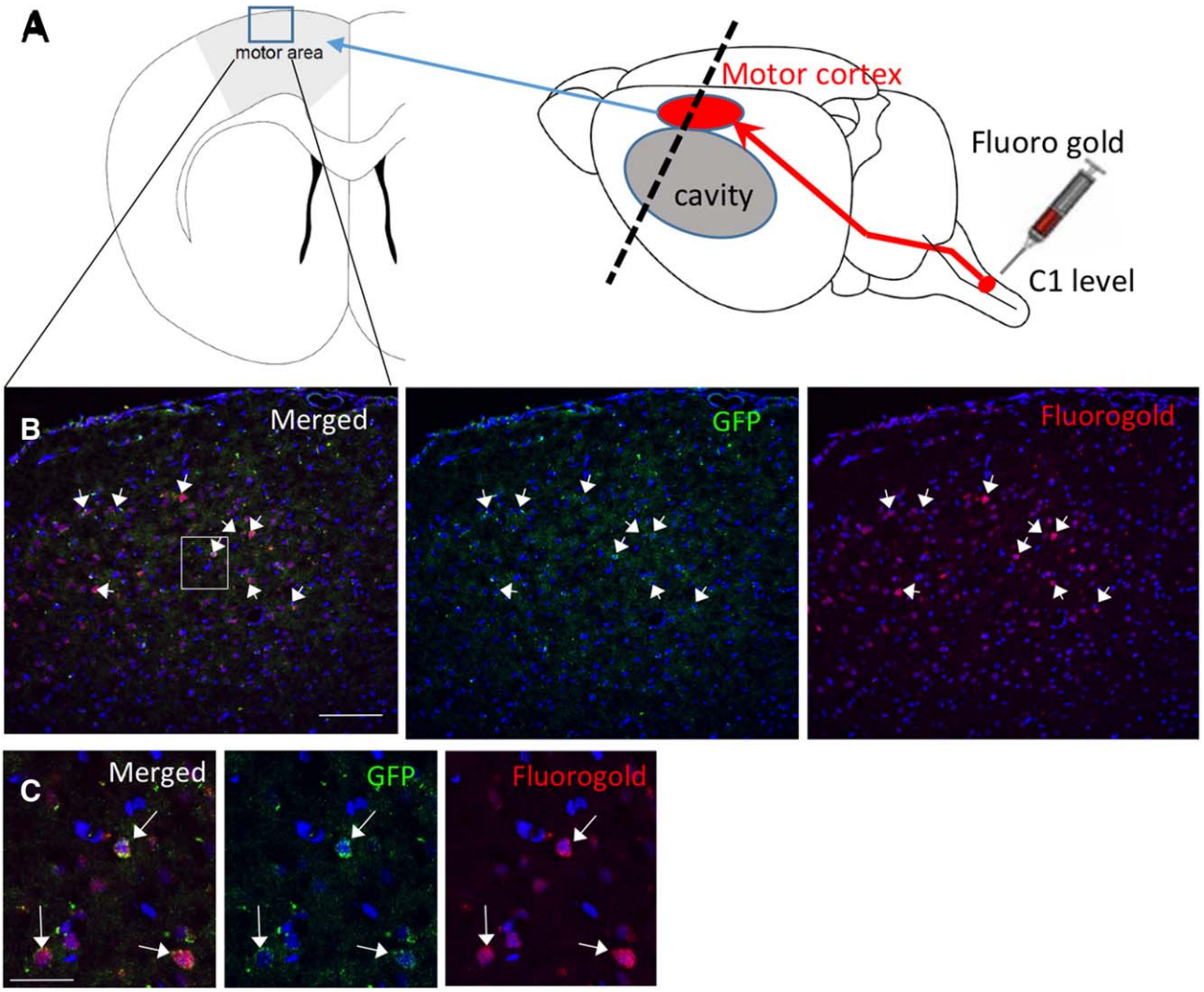

Figure 5. Retrograde labeling of Muse cells that integrated into the motor cortex. **(A)**: Schematic diagram illustrating the injection site of the fluorogold at contralateral dorsal funiculus of cervical spinal cord (C1 level) at 84 days after transplantation and the site of detection at the ipsilateral motor cortex at day 91. **(B)**: Fluorescent staining with fluorogold (red) and GFP (green) revealed that GFP+-Muse cells in the ipsilateral motor cortex were retrogradely labeled by fluorogold (arrows). Scale bar = 100 μm. **(C)**: Enlarged image of the white rectangular box in (B). Arrows indicate double-positive cells. Scale bar = 50 μm. Abbreviation: GFP, green fluorescent protein.

integrated with the stroke tissue spontaneously differentiated into neuronal- (NeuN, MAP-2, and calbindin) and oligodendrocyte (GST-π)-positive cells. An equally major finding here is the unprecedented good graft survival and long-term engraftment of Muse cells, detected either by GFP or hMit, in the stroke peri-infarct area as well as in the sensory and motor cortex at least up to day 84 post-transplantation, while graft persistence was not detected in the vast majority of transplanted non-Muse cells, altogether suggesting that Muse cells were more stress tolerant and could survive better in the hostile stroke environment than non-Muse cells. Concomitant with their robust stemness and transplantable cell properties, grafted Muse cells also exerted substantial improvements in both neurological and motor functions at the chronic stroke stage of days 70 and 84. Although infarct size was not reduced, transplantation of Muse cells increased host cell survival within the peri-infarct area. Because infarct volume quickly peaks within hours after ischemic stroke onset, the early timing of cell transplantation will be critical in abrogating the infarct volume. Additional studies, with transplant initiation at supra acute time post-stroke, are warranted to recognize the potential of Muse cell transplantation in reducing the infarct volume. Notwithstanding, the series of regenerative events that Muse cells underwent prior to affording functional recovery, namely host integration of the cells, differentiation into neural cells, extension of neurites, and reconstruction of the neural circuitry, likely occurred over a period of time, which delayed the recognition of behavioral effects not until the chronic stroke phase. To this end, Muse cells that integrated into the motor cortex extended their neurites at least to the dorsal funiculus of the cervical spinal cord, suggesting their commitment to augment pyramidal tract functions, which seems to be consistent with the observed robust behavioral recovery in mNSS and rotarod test. Moreover, Muse cells that engrafted into the sensory cortex possibly also incorporated into the somatosensory circuitry that was spared from the stroke insult, facilitating the normalization of SEPs. Finally,

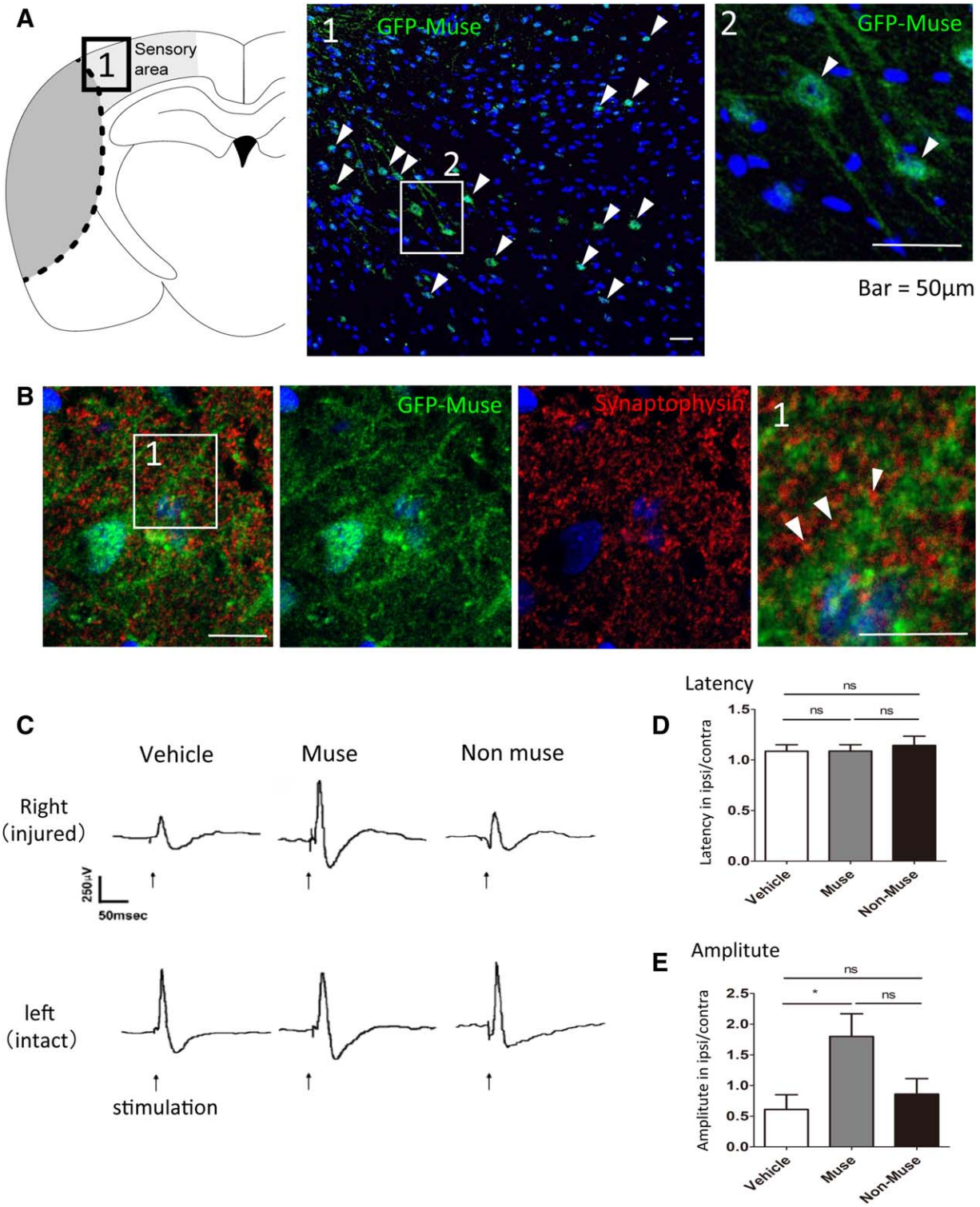

Figure 6. Quantitative analysis of electrophysiologic data 84 days after transplantation. **(A)**: GFP+-Muse cells detected at the ipsilateral sensory cortex at day 84 (arrowheads). 1 and 2 are enlarged images of each corresponding box areas. Scale bar = 50 μm. **(B)**: Synaptophysin (red) was detected adjacent to dendrite-like structure of GFP+ Muse cells (green) in the sensory cortex (arrowheads). Scale bar = 10 μm. **(C)**: Representative somatosensory evoked potentials (SEP) in the vehicle, Muse, and non-Muse groups. **(D, E)**: Ratio of SEP latency on ipsilateral side to that on contralateral side (D) and ratio of SEP amplitude on ipsilateral side to that on contralateral side (E). Significant difference was recognized between the two groups. *, $p < .05$. Abbreviation: GFP, green fluorescent protein.

the grafted Muse cell fate commitment to neural lineage, its persistence and integration with stroke brain and somatosensory pathway, and its therapeutic outcomes were not associated with any observable tumor formation or overt behavioral abnormalities for up to 84 days post-transplantation.

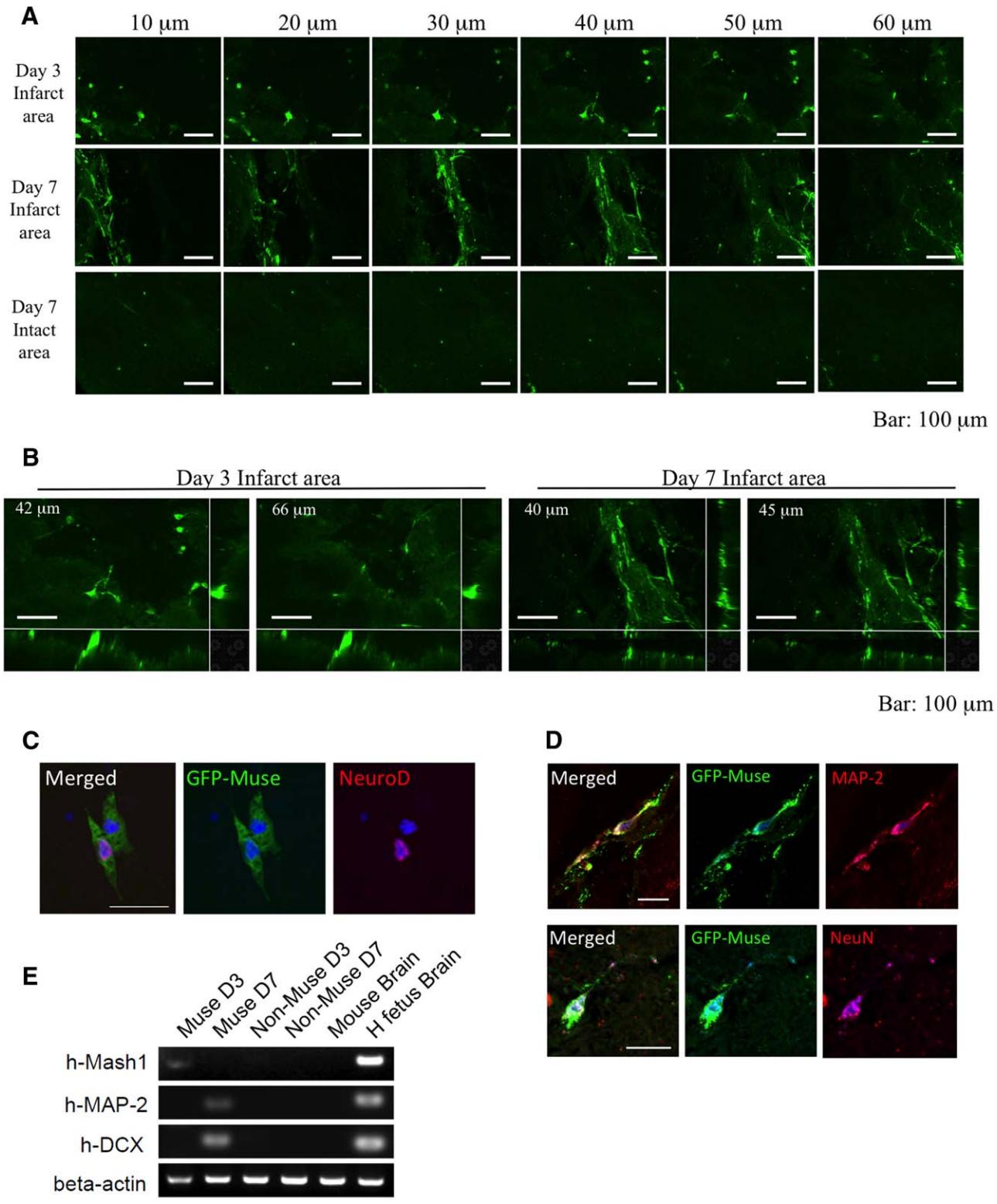

Figure 7. Reponses of Muse cells to stroke microenvironmental cues. **(A, B)**: Multiphoton laser microscopic images obtained in every 10 μm. GFP+-Muse cells penetrated into the SCID mouse brain slices and extended neurite-like processes at day 3. Day 7 shows connection-like organization of elongation of processes. In contrast, day 7 at intact area did not show integration of GFP+-Muse cells. Bars = 100 μm. **(C)**: NeuroD expression in GFP+-Muse cells. Section obtained from the sample of "day 3 infarct area" in (A). Bar = 50 μm. **(D)**: MAP-2 and NeuN expression in GFP-Muse cells in "day 7 infarct area" in (A). Bar = 50 μm. **(E)**: RT-PCR of the cocultured stroke brain slices. Beta actin of mouse brain is from mouse beta actin signal, and the remainder of samples is from human beta actin signal. Human Mash1, human MAP-2, and human DCX were only detectable in Muse-stroke brain slice (day 3 and day 7). Abbreviation: GFP, green fluorescent protein.

Although dermal fibroblasts are commonly considered terminally differentiated cells, some reports suggest that they contain a subset of cells with high differentiation potential [22–25]. Such a subpopulation, however, remained to be well-identified and characterized. Fibroblast transplantation in ischemic stroke has generally been used as a negative control for evaluating the effects of stem cell therapies, demonstrating that transplantation of fibroblasts, even in a large bulk, showed no beneficial effects on the damaged brain [26]. Consistent with these findings, non-Muse cells, representing the major subset of the fibroblasts, neither engrafted in the host tissue nor improved behavioral outcomes in this study. Although bulk fibroblasts comprise several percent of Muse cells and vast majority of non-Muse cells may mask the robust effects of Muse cells in such nonselective fibroblast transplantation. Our results demonstrated that fibroblasts pose as efficacious candidate transplantable cells for treating stroke if their Muse cells are fully used by purification and enrichment (i.e., targeted to injured microenvironment).

Similar to fibroblast-derived Muse cells, human BM-derived Muse cells transplanted into immunodeficient stroke mice also demonstrated that only Muse cells engrafted in the host brain and spontaneously differentiated into neuronal (Tuj-1 and NeuN) and glial (GFAP) marker-positive cells at 5 weeks, while such effect was not observed in non-Muse cell transplantation [14]. Since the endpoint was set at 5 weeks, earlier than this study, substantial functional recovery could not be recognized in this BM-derived Muse cell transplantation study [14]. Oligodendrocyte (GST-π)-positive cells, but not astrocyte (GFAP)-positive cells were detected in our study, as opposed to the previous study, may be related to progressive cell death events during chronic stroke phase allowing a dynamic set of microenvironmental cues to influence the eventual cell fate of Muse cells. This speculation is an interesting issue that warrants future investigations.

While Muse cells, a small subset of fibroblasts, are classified as somatic stem cells, they are apparently unique in their potential. Human somatic stem cells typically generate cell types of the tissue in which they reside, thus the range of their differentiation capacities is considered limited [27]. In this regard, fetal neural stem cells appear to be more suitable for replacing lost neural circuitry, considering their preferential differentiation toward the neural lineage [7, 28], but their limited accessibility and expansion capacity may be problematic for an adequate clinical supply. Even if they are not manipulated cells, like embryonic stem cells and iPS cells, their immature properties may present with safety issues. In fact, the formation of donor-derived tumors was reported in a clinical study of neural stem cell transplantation for an ataxia telangiectasia patient [29]. Similarly, manipulated cells, such as neuronal cells derived from ESCs or iPS cells, which may require treatment with oncogenic factors or cocktail of growth factors, while promising candidates for the treatment of ischemic stroke are plagued with several safety issues and ethical concerns that must be resolved before they can be applied in a clinical setting [30–32]. Another possible source for neural cells is MSCs; they are nontumorigenic, but they are heterogeneous and, like nonselective fibroblasts, bulk MSCs are reported to show moderate efficiency in differentiating into the neural lineage cells both in vitro and in vivo if they are used in a naive state [4, 33–36]. Although further in-depth evaluation is still necessary, including vis-à-vis comparisons between these stem cell types, our results suggest that fibroblast-derived Muse cells stand as efficacious transplantable cells for ischemic stroke, circumventing many of the ethical and logistical obstacles inherent in cell therapy.

Acute cell delivery within the 48 hours postinjury often reduces lesion size and attenuate apoptosis in the penumbra, suggesting an important role of cell-induced neuroprotection in facilitating recovery [2, 4, 17, 37]. Moreover, accumulating evidence indicates that cell therapies can enhance many endogenous repair processes, such as vascular regeneration and induction of host brain plasticity, that occur after stroke [4, 37]. Conversely, evidence that stem cell therapies replace lost circuitry is limited. Some studies demonstrated that transplanted neural stem cells form synapses with host circuitry and exhibit electrophysiological properties, reminiscent of functional neurons [7, 38]. Only a few synapses were observed, however, and recovery occurred too early to be attributable to newly formed neuronal connections [39], implying that neuronal replacement is not a major contributor to cell-induced recovery. In this study, functional improvement was observed at the chronic stroke stage, coupled with good graft survival and long-term engraftment in the ischemic cortex with extensive neurite processes incorporating into the pyramidal tract and possibly into the somatosensory circuitry. Although Muse cells did not reduce infarct size, host survival within the peri-infarct area was preserved, indicating limited neuroprotection. Notwithstanding, this data suggest that Muse cells exerted therapeutic benefits in stroke mainly through reconstruction of the damaged neuronal circuitry with partial trophic effects. Because trophic effects are generally acute and transient, the observed graft persistence and neuronal circuitry reconstruction in chronic stroke may translate into more stable and long-lasting functional outcomes.

Conclusions

Muse cells have practical advantages for regenerative medicine; they are nontumorigenic, easily accessed both commercially and from skin biopsies of patients, and can be easily collected as SSEA-3(+) cells either by FACS or magnetic-activated cell sorting [10]. Most importantly, Muse cells do not need to be induced to attain stemness and to commit into specific lineages prior to transplantation, because they already display inherent stem cell properties upon isolation, and after transplantation spontaneously home into the damaged site and differentiate into cells compatible with the target tissue, rendering the need for gene manipulation and intricate cell induction protocols unnecessary [10]. They can rigorously repair the stroke brain simply by two steps, namely collection from fibroblasts and transplantation to the damaged tissue. This study was conducted with small number of Muse cells, namely 30,000 cells, compared to general MSC transplantation experiments, demonstrating their high

regenerative performances. Muse cells are thus a feasible and promising cell source for stem cell-based approaches to ischemic stroke therapy.

Author Contributions

H.U., T.M., Y.Kushida, Y.Kuroda, S.W., Y.M., and H.M.: collection and/or assembly of data; K.N. and H.S.: data analysis and interpretation; T.T.: financial support and data analysis and interpretation; C.V.B.: conception and design, data analysis and interpretation, and manuscript writing; M.D.: conception and design, financial support, administrative support, data analysis and interpretation, and manuscript writing. H.U. and T.M. contributed equally to this article.

Disclosure of Potential Conflicts of Interest

Hiroki Uchida, Takahiro Morita, Yoshihiro Kushida, Yasumasa Kuroda, Shohei Wakao, and Mari Dezawa of Department of Stem Cell Biology and Histology, Tohoku University Graduate School of Medicine, and Hiroyuki Sakata, Kuniyasu Niizuma, and Teiji Tominaga of Department of Neurosurgery, Tohoku University Graduate School of Medicine, which are parties to a codevelopment agreement concluded with Clio, Inc. under subsidy from the New Energy and Industrial Technology Development Organization.

Acknowledgment

This work was supported by the grant aid of the New Energy and Industrial Technology Development Organization (NEDO).

References

1 Abe K, Yamashita T, Takizawa S et al. Stem cell therapy for cerebral ischemia: From basic science to clinical applications. J Cereb Blood Flow Metab 2012;32:1317–1331.

2 Lindvall O, Kokaia Z. Stem cell research in stroke: How far from the clinic? Stroke 2011;42:2369–2375.

3 Chen J, Li Y, Wang L et al. Therapeutic benefit of intravenous administration of bone marrow stromal cells after cerebral ischemia in rats. Stroke 2001;32:1005–1011.

4 Chen J, Zhang ZG, Li Y et al. Intravenous administration of human bone marrow stromal cells induces angiogenesis in the ischemic boundary zone after stroke in rats. Circ Res 2003;92:692–699.

5 Parr AM, Tator CH, Keating A. Bone marrow-derived mesenchymal stromal cells for the repair of central nervous system injury. Bone Marrow Transplant 2007;40:609–619.

6 Honmou O, Houkin K, Matsunaga T et al. Intravenous administration of auto serum-expanded autologous mesenchymal stem cells in stroke. Brain 2011;134:1790–1807.

7 Bliss TM, Andres RH, Steinberg GK. Optimizing the success of cell transplantation therapy for stroke. Neurobiol Dis 2010;37:275–283.

8 Shen LH, Li Y, Chen J et al. One-year follow-up after bone marrow stromal cell treatment in middle-aged female rats with stroke. Stroke 2007;38:2150–2156.

9 Takahashi K, Yamanaka S. Induction of pluripotent stem cells from mouse embryonic and adult fibroblast cultures by defined factors. Cell 2006;126:663–676.

10 Kuroda Y, Kitada M, Wakao S et al. Unique multipotent cells in adult human mesenchymal cell populations. Proc Natl Acad Sci USA 2010;107:8639–8643.

11 Wakao S, Kitada M, Kuroda Y et al. Multilineage-differentiating stress-enduring (Muse) cells are a primary source of induced pluripotent stem cells in human fibroblasts. Proc Natl Acad Sci USA 2011;108:9875–9880.

12 Kuroda Y, Wakao S, Kitada M et al. Isolation, culture and evaluation of multilineage-differentiating stress-enduring (Muse) cells. Nat Protoc 2013;8:1391–1415.

13 Kinoshita K, Kuno S, Ishimine H et al. Therapeutic potential of adipose-derived SSEA-3-positive muse cells for treating diabetic skin ulcers. Stem Cells Transl Med 2015;4:146–155.

14 Yamauchi T, Kuroda Y, Morita T et al. Therapeutic effects of human multilineage-differentiating stress enduring (MUSE) cell transplantation into infarct brain of mice. PLoS One 2015;10:e0116009.

15 Ogura F, Wakao S, Kuroda Y et al. Human adipose tissue possesses a unique population of pluripotent stem cells with nontumorigenic and low telomerase activities: Potential implications in regenerative medicine. Stem Cells Dev 2014;23:717–728.

16 Hayase M, Kitada M, Wakao S et al. Committed neural progenitor cells derived from genetically modified bone marrow stromal cells ameliorate deficits in a rat model of stroke. J Cereb Blood Flow Metab 2009;29:1409–1420.

17 Sakata H, Niizuma K, Yoshioka H et al. Minocycline-preconditioned neural stem cells enhance neuroprotection after ischemic stroke in rats. J Neurosci 2012;32:3462–3473.

18 Matsuse D, Kitada M, Kohama M et al. Human umbilical cord-derived mesenchymal stromal cells differentiate into functional Schwann cells that sustain peripheral nerve regeneration. J Neuropathol Exp Neurol 2010;69:973–985.

19 Matsuse D, Kitada M, Ogura F et al. Combined transplantation of bone marrow stromal cell-derived neural progenitor cells with a collagen sponge and basic fibroblast growth factor releasing microspheres enhances recovery after cerebral ischemia in rats. Tissue Eng Part A 2011;17:1993–2004.

20 Mimura T, Dezawa M, Kanno H et al. Behavioral and histological evaluation of a focal cerebral infarction rat model transplanted with neurons induced from bone marrow stromal cells. J Neuropathol Exp Neurol 2005;64:1108–1117.

21 Leergaard TB, Alloway KD, Pham TA et al. Three-dimensional topography of corticopontine projections from rat sensorimotor cortex: Comparisons with corticostriatal projections reveal diverse integrative organization. J Comp Neurol 2004;478:306–322.

22 Chen FG, Zhang WJ, Bi D et al. Clonal analysis of nestin(-) vimentin(+) multipotent fibroblasts isolated from human dermis. J Cell Sci 2007;120:2875–2883.

23 Lorenz K, Sicker M, Schmelzer E et al. Multilineage differentiation potential of human dermal skin-derived fibroblasts. Exp Dermatol 2008;17:925–932.

24 Shi CM, Cheng TM. Differentiation of dermis-derived multipotent cells into insulin-producing pancreatic cells in vitro. World J Gastroenterol 2004;10:2550–2552.

25 Toma JG, Akhavan M, Fernandes KJ et al. Isolation of multipotent adult stem cells from the dermis of mammalian skin. Nat Cell Biol 2001;3:778–784.

26 Liu Y, Kim D, Himes BT et al. Transplants of fibroblasts genetically modified to express BDNF promote regeneration of adult rat rubrospinal axons and recovery of forelimb function. J Neurosci 1999;19:4370–4387.

27 Korbling M, Estrov Z. Adult stem cells for tissue repair—A new therapeutic concept? N Engl J Med 2003;349:570–582.

28 Kelly S, Bliss TM, Shah AK et al. Transplanted human fetal neural stem cells survive, migrate, and differentiate in ischemic rat cerebral cortex. Proc Natl Acad Sci USA 2004;101:11839–11844.

29 Amariglio N, Hirshberg A, Scheithauer BW et al. Donor-derived brain tumor following neural stem cell transplantation in an ataxia telangiectasia patient. PLoS Med 2009;6:e1000029.

30 Erdo F, Buhrle C, Blunk J et al. Host-dependent tumorigenesis of embryonic stem cell transplantation in experimental stroke. J Cereb Blood Flow Metab 2003;23:780–785.

31 Kawai H, Yamashita T, Ohta Y et al. Tridermal tumorigenesis of induced pluripotent stem cells transplanted in ischemic brain. J Cereb Blood Flow Metab 2010;30:1487–1493.

32 Seminatore C, Polentes J, Ellman D et al. The postischemic environment differentially impacts teratoma or tumor formation after transplantation of human embryonic stem cell-derived neural progenitors. Stroke 2010;41:153–159.

33 Tang Y, Yasuhara T, Hara K et al. Transplantation of bone marrow-derived stem cells: A promising therapy for stroke. Cell Transplant 2007;16:159–169.

34 Borlongan CV, Glover LE, Tajiri N et al. The great migration of bone marrow-derived stem cells toward the ischemic brain: Therapeutic implications for stroke and other neurological disorders. Prog Neurobiol 2011;95:213–228.

35 Xin H, Li Y, Cui Y et al. Systemic administration of exosomes released from mesenchy-

mal stromal cells promote functional recovery and neurovascular plasticity after stroke in rats. J Cereb Blood Flow Metab 2013;33: 1711–1715.
36 Chen J, Venkat P, Zacharek A et al. Neurorestorative therapy for stroke. Front Hum Neurosci 2014;8:382.
37 Sakata H, Narasimhan P, Niizuma K et al. Interleukin 6-preconditioned neural stem cells reduce ischaemic injury in stroke mice. Brain 2012;135:3298–3310.
38 Buhnemann C, Scholz A, Bernreuther C et al. Neuronal differentiation of transplanted embryonic stem cell-derived precursors in stroke lesions of adult rats. Brain 2006;129: 3238–3248.
39 Englund U, Bjorklund A, Wictorin K et al. Grafted neural stem cells develop into functional pyramidal neurons and integrate into host cortical circuitry. Proc Natl Acad Sci USA 2002;99:17089–17094.


See www.StemCells.com for supporting information available online.

